

# Two-photon pumped zinc oxide random laser

E.V. Chelnokov<sup>a, b\*</sup>, N.M. Bityurin<sup>b</sup>, W. Marine<sup>a</sup>

<sup>a</sup> Centre de Recherche en Matière Condensée et Nanosciences CNRS, Marseille, France

<sup>b</sup> Institute of Applied Physics, Russian Academy of Sciences, 603950 Nizhny Novgorod, Russia

## ABSTRACT

Zinc oxide is a promising material for creation of novel ultraviolet light sources. In this work we study random laser action in a thin ZnO nanocluster film under two-photon pumping. The results are compared with the case of single-photon pumping. A theoretical model is developed, which shows the effect of boundary conditions on lasing in the film. Measurement results of nonlinear transmission are presented and compared with classical two-photon absorption model.

**Keywords:** zinc oxide (ZnO), nanocluster, two-photon pumping, random laser, pulsed laser deposition, ultraviolet (UV), boundary conditions.

## 1. INTRODUCTION

Wide-bandgap semiconductors have recently attracted interest for their applications in solid-state electronics and optics. Zinc oxide (ZnO) is a II-VI semiconductor with a wide bandgap of 3.37 eV and high exciton binding energy of 60 meV allowing its applications at room- and higher temperatures. Moreover, recently it has been observed that a nanostructured ZnO thin film exhibits very high optical nonlinear properties<sup>1</sup>. ZnO has a relatively high refractive index 2.6, which provides high reflection from the ZnO-air interface.

A random laser uses a highly disordered structure to obtain laser action. Instead of bouncing from one mirror to another, the light waves bounce from one particle to another thousand of times before they leave the disordered material<sup>2</sup>. However, multiple scattering alone is not sufficient to make a laser. A laser requires two ingredients: a material that amplifies light, and some feedback mechanism that (temporarily) traps the light for the amplification to be efficient. In normal lasers the trapping element is a cavity – two mirrors facing each other with the amplifying material in between. In the case of a random laser the cavity is replaced by multiple scattering. In 1968, Letokhov predicted that the combination of multiple scattering and light amplification would lead to a form of laser action<sup>3</sup>. The emission characteristics of a random laser are similar to those of a normal laser: the emission spectrum can be extremely narrow, which means that the colour of the emission is well defined, and the output can be pulsed. But unlike a regular laser, a random laser will emit randomly in all directions, just like the emission from a common light bulb.

Random laser effect is well known in colloidal and microsized media from experimental point of view<sup>4</sup>. But studies in the case of nanostructured materials are not so well advanced because of the lack of pure and size controlled ZnO nanocluster materials. In this communication, we present excellent optical properties of nanoclusters, prepared by the pulsed laser ablation method<sup>5</sup>. Well controlled nanostructured ZnO thin films allow easy observation of random laser effect under single photon or multiple photon excitation. In both cases we used femtosecond (130 fs) optical parametric amplifier as a pumping source. Excitation wavelengths were 350, 700 nm.

Dependences of emission intensity, spectral width and spectral position of random laser emission on pump laser fluence have been studied for various ZnO films.

The results of single- and two-photon pumping spectra treatment are compared. The linear (350 nm) and quadratic (700 nm) dependences of laser output intensities on pumping fluence confirm participation of single- and two-photon pumping, respectively. It is shown that the ratio of damage and laser action thresholds is higher for single photon pumping than for two-photon pumping

---

\* Corresponding author: [che@ufp.appl.sci-nnov.ru](mailto:che@ufp.appl.sci-nnov.ru),

<sup>a</sup> [www.crmcn.univ-mrs.fr](http://www.crmcn.univ-mrs.fr),

<sup>b</sup> [www.iapras.ru](http://www.iapras.ru)

A strong increase of the laser action threshold with a decrease of laser beam area was observed. The value of threshold fluence tends to a constant with increasing area of the spot. The experimental results on spot dependence of laser action threshold were compared with the prediction of Letokhov's theory applied to disordered films.

The effective cavity length was estimated from a period of laser modes of output spectra obtained with high resolution.

The transmission of the nanostructured ZnO films during the two-photon pumping experiments was investigated as a function of the intensity of pumping pulses. Saturation in transmission decrease with increasing pumping fluence was observed.

## 2. MATERIALS AND METHODS

Nanoclusters of ZnO were prepared by means of the "pulsed laser deposition" technique<sup>5</sup>. This method allows one to produce nanoclusters of high purity and to control their size. In this work we present a random laser on particles of zinc oxide with the size of 5-10 nm.

Photoluminescence and transmission spectra of a ZnO film are shown in fig. 1. From the first one we estimate the band gap. Exciton peak position corresponds to the emission wavelength. The ratio of the exciton peak amplitude to the peak of defects and impurities (500-550 nm) gives information about quality<sup>6</sup> of nanocluster film.

The experimental scheme is shown in fig. 2. The system consists of "Mai-Tai" generator, "Hurricane" amplifier and optical parametric amplifier (OPA) which allows changing the pumping wavelength, for example, for two-photon excitation.

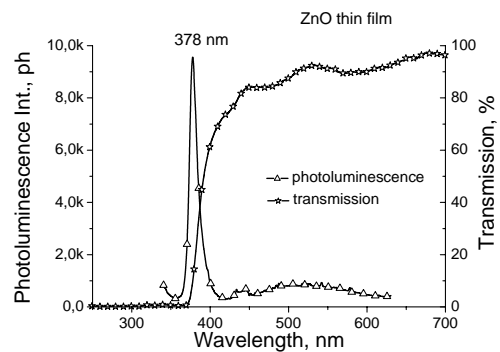


Fig. 1. ZnO film photoluminescence and transmission spectra.

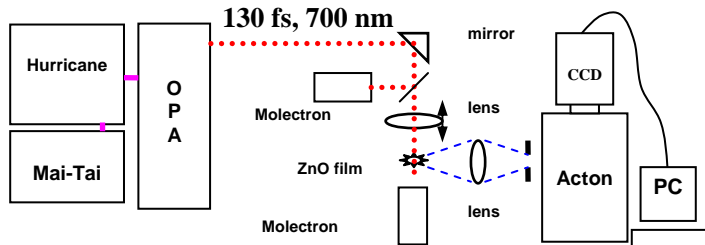


Fig. 2. Experimental scheme.

The laser pulse with duration 130 fs and wavelength 350 nm (700 nm) is focused perpendicular to the surface of the film. The incident energy is measured by "Molelectron" energy-meter. The photoluminescence emission signal is collected to the spectrometer slit in a plane of the film. The spectrometer signal is detected by a CCD camera and transferred to the computer.

In the case of two-photon excitation transmission experiment is also possible in this setup.

## 3. RESULTS AND DISCUSSION

### 3.1. Two-photon pumping

Despite the recent achievements in single-photon pumping<sup>4, 11, 12</sup> it cannot be recognized as the best one. For the photons more energetic than a band gap, the absorption coefficient is extremely high  $\alpha_{350 \text{ nm}} \approx 10^5 \text{ cm}^{-1}$ . It corresponds to the light penetration depth  $l_{ab} \sim 100 \text{ nm}$ . This means that for a 1  $\mu\text{m}$  thick film all pumping energy is absorbed near the surface. On the contrary, in the case of pumping by two-times weaker photon, characteristic length of absorption is much greater. Thus, there is a possibility to pump over all sample's thickness. It may be favourable for some applications.

Secondly, wavelengths of excitation and emission are too close to separate in the case of single-photon pumping (350 and 375 nm). Two-photon pumping wavelength is strongly distinct from emission wavelength (700 and 375 nm).

At the moment, there are no experimental works on two-photon pumping of ZnO. We were the first to study infrared (IR) pumping of ZnO.

Changes of emitted spectra as a function of pumping fluence (pulse energy density) are shown in fig. 3 for the two-photon pumping case. The spectra clearly show lasing modes. Using expression (1) for the Fabri-Perot resonator and the function  $n(\lambda)$  a cavity length of random resonator is found:

$$\Delta\lambda = \frac{\lambda^2}{2\ell \cdot (n - \lambda_0 \frac{dn}{d\lambda})}, \quad (1)$$

The resonator length  $\ell$  is approximately 20  $\mu\text{m}$ . This result is in agreement with [8].

Depending on pumping energy, the peak of the laser effect increases, changing its position and becoming wider. The stronger peak can be fitted with two Gaussians to underline its asymmetry. These peaks correspond to two known mechanisms of recombination: exciton-exciton collision and electron-hole plasma recombination<sup>9</sup>.

Results of single- and two-photon pumping are compared in fig. 4. The linear (open square) and quadratic (open circle) dependences of lasers intensities versus pumping fluence can be considered as the ratio between the number of absorbed and emitted photons. Thus, this confirms single and two-photon pumping, respectively. The laser action threshold corresponds to narrowing of luminescence peak.

The ratio of damage thresholds confirms that the films have different heating (damage) mechanisms. Also, it is obvious that the ratio of the damage and laser effect thresholds is higher for single-photon pumping. Thus, from this point of view single-photon pumping is advantageous.

### 3.2. Single-photon pumping

The photoluminescence spectra near the threshold of laser effect in ZnO nanoparticles film under single-photon pumping are shown in fig. 5 for different pumping energies.

When the pumping energy is a little bit higher than the threshold energy on the base of a wide luminescence peak ( $\Delta_1 \sim 20$  nm), a weaker peak ( $\Delta_2 \sim 3.6$  nm) of laser effect appears. The existence of laser modes from the curve for higher pumping energy is obvious.

The measured threshold versus spot radius is plotted in Fig. 9. This behaviour of the dependence requires careful theoretical analyses which are different for the case of single- and two-photon pumping<sup>4</sup> because of the difference in absorption depth of pumping light. Qualitatively, the existence of minimum in the spot size corresponds to the least spot size  $\sim 30$   $\mu\text{m}$  when the generation is possible<sup>10</sup> i. e., to the resonator length. When the pumped area size is increased, the lasing threshold decreases to a minimally allowable value and then does not change with any further increase<sup>11</sup> (fig. 9, a). This can be attributed to the existence of a laser action threshold that is independent of spot size and is determined by sample properties only.

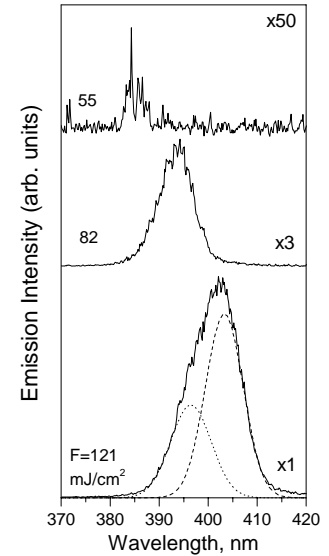


Fig. 3. Emission spectra from ZnO thin film. The spectra are shifted vertically for clarity. The pumping fluences are marked on the left.

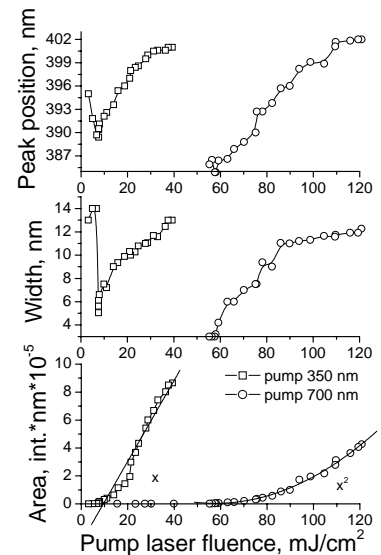


Fig. 4. Comparison of single- & two-photon pumping.

### 3.3. Nonlinear absorption

As was said earlier, under two-photon pumping, the sample is illuminated over its entire thickness. Therefore, the experiment for measurement of two-photon transmission can be conducted by the scheme depicted in fig. 2. Figure 6 demonstrates experimental values of the dependence of ZnO nanocluster film transmission on pump intensity.

The solution of the two-photon transmission equation  $\partial I / \partial x = -\delta n_0 I^2$  is a hyperbolic function  $T = (1 + \delta n_0 I_0 L)^{-1}$ , where  $\delta$  is the two-photon absorption cross-section,  $n_0$  is the electron concentration,  $I_0$  is the laser intensity at the outer boundary of the medium, and  $L$  is the sample thickness. The fit between experimental and theoretical curves may be considered to be satisfactory only at small intensities  $I_0 < 20 \text{ GW/cm}^2$ . At high intensities, nonlinear transmission saturation occurs, resulting in the discrepancy between experimental and theoretical data.

Can the curve saturation be attributed to valence band depletion? Knowing pulse energy and band gap width, we obtain that the maximum value of free electron concentration in the conduction band is  $n_{free}^{max} \approx 10^{19} \text{ cm}^{-3}$ . The concentration of valent electrons in ZnO is  $n_{valent}^{ZnO} \approx 10^{23} \text{ cm}^{-3}$ . Thus we obtain  $n_{free}^{max} \ll n_{valent}^{ZnO}$ . Hence, the valence band depletion approach cannot explain the transmission saturation observed in our experiment.

The saturation can be explained by over-population of the impurity/defect level in the band gap. In this case the nonlinear transmission has a two-step nature.

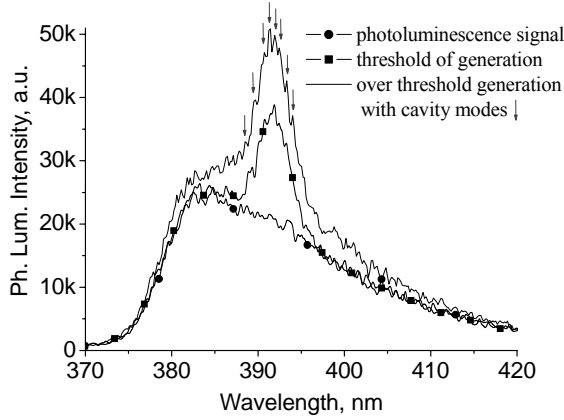


Fig. 5. Photoluminescence and laser effect threshold for ZnO nanocluster thin film under 350 nm pumping.

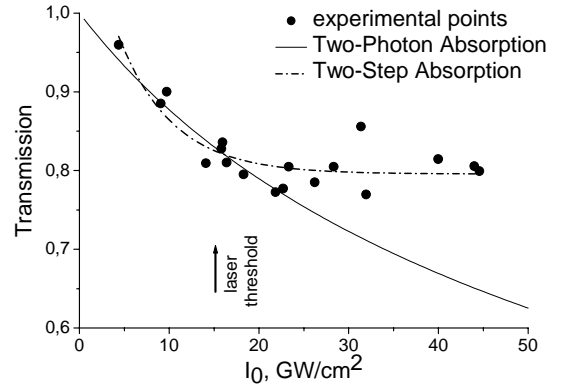


Fig. 6. Experimental and theoretical nonlinear transmission curves.

## 4. THEORETICAL MODEL

### 4.1. Random lasing in disordered films. Setting of the problem

To explain the experimental dependence of laser action threshold on diameter of pumping beam we consider a plane film of disordered medium of thickness  $2z_0$  with effective refractive index  $n_2$ , surrounded by a medium with refractive index  $n_1$  (air) and a medium with refractive index  $n_3$  (substrate) fig. 7. Pumping is provided by the laser beam with diameter  $2r_0$ . We assume that the pumping intensity is constant within the cylinder:  $r < r_0$ ,  $-z_0 < z < z_0$ . The propagation of the emitted light within the medium can be described by the diffusion equation with gain<sup>3,12</sup>.

$$\frac{\partial I}{\partial t} = D\Delta_{\perp} I + D \frac{\partial^2 I}{\partial z^2} + gI, \quad (2)$$

$$D \frac{\partial I}{\partial z} \Big|_{z=z_0} = -\alpha_1 I(r, z_0), \quad (3)$$

$$D \frac{\partial I}{\partial z} \Big|_{z=-z_0} = \alpha_2 I(r, -z_0). \quad (4)$$

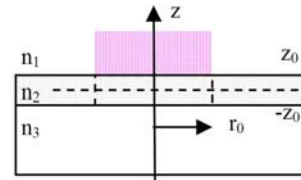


Fig. 7. Geometry of the thin film sample.

Here  $I$  is the intensity ( $I=Uv$ , where  $U$  is the photon density and  $v$  is the light velocity in the medium),  $D$  is the light diffusion coefficient in the medium ( $D = v l^* / 3$  where  $l^*$  is the transport mean free path of the light in the scattering medium),  $g$  is gain that is determined by the pumping. Boundary conditions (3)-(4) take into account the effect of reflection of light at the boundaries of the active medium. Boundary conditions at  $r = r_0$  are not very important and we choose them to be

$$I(r_0, z) = 0. \quad (5)$$

According to the theory of Letokhov<sup>3,12</sup>, generation of random laser corresponds to existence of a solution of the set (2)-(5) that is exponentially growing in time. The substitution of solution in the form  $I(r, z, t) = \exp(\lambda t) \bar{I}(r, z)$  gives

$$\lambda \bar{I} = D \Delta_{\perp} \bar{I} + D \frac{\partial^2 \bar{I}}{\partial z^2} + g \bar{I}. \quad (6)$$

Generation corresponds to the existence of eigen-function of the problem (6), (3)-(5) with eigen-value  $\lambda \geq 0$ . The variables in the considered problem (6), (3)-(5) are separating. It means that we can find solution in the form:  $\bar{I}(r, z) = I_r(r) I_z(z)$ .

Equation for the radial part reads as

$$D \Delta_{\perp} I_r(r) + \bar{b}^2 I_r(r) = 0, \quad (7)$$

$$I_r(r_0) = 0, \quad (8)$$

Equation for the  $z$ -part reads as

$$D \frac{\partial^2 I_z(z)}{\partial z^2} + \bar{a}^2 I_z(z) = 0, \quad (9)$$

$$D \frac{\partial I_z}{\partial z} \Big|_{z=z_0} = -\alpha_1 I_z(z_0), \quad (10)$$

$$D \frac{\partial I_z}{\partial z} \Big|_{z=-z_0} = \alpha_2 I_z(-z_0). \quad (11)$$

The condition of generation  $\lambda \geq 0$  becomes:

$$g \geq \bar{a}^2 + \bar{b}^2. \quad (12)$$

The task is to find the minimal values of  $\bar{b}^2$  and  $\bar{a}^2$  from the eigen-value problems (7)-(8) and (9)-(11).

## 4.2. Solution of the eigen-value problems

The solution of the problem (7)-(8) yields:

$$\bar{b}^2 = D j_{01}^2 / r_0^2, \quad (13)$$

where  $j_{01}$  is the first root of the Bessel function. Let us consider the problem (9)-(11). The case  $\alpha_1 / D \rightarrow \infty$  corresponds to the boundary condition  $I_z(z_0) = 0$ . This is the case of absence of any reflection at the boundary. This condition is the most frequently used one in the theory of random lasers<sup>12</sup>. If  $\alpha_1 / D \rightarrow 0$ , one comes to the condition  $(\partial I_z / \partial z) \Big|_{z=z_0} = 0$ . This corresponds to the existence of an ideal mirror at the surface  $z = z_0$ . Similarly,  $\alpha_2 / D \rightarrow \infty$  leads

to  $I_z(-z_0) = 0$  and  $\alpha_2 / D \rightarrow 0$  means that  $(\partial I_z / \partial z) \Big|_{z=-z_0} = 0$ . The latter puts an ideal mirror at the surface  $z = -z_0$ .

### 4.2.1. Symmetrical case

It is useful to start consideration of the problem (9)-(11) with the symmetrical case  $\alpha_1 = \alpha_2 = \alpha$ .

The solution of equation (9) is

$$I_z = \cos(az), \quad a^2 = \bar{a}^2 / D. \quad (14)$$

The boundary condition (10), which for the symmetrical case reads  $D(\partial I_z / \partial z)|_{z=z_0} = -\alpha I_z(z_0)$ , after introducing  $x \equiv az_0$  and  $p \equiv D/\alpha z_0$  yields the following equation:

$$ctg(x) = px. \quad (15)$$

When  $p = 0$  ( $\alpha/D \rightarrow \infty$ , no reflection from the boundaries),  $x = \pi/2$ . It means that

$$a = \frac{\pi}{2z_0}, \quad \bar{a}^2 = D \frac{\pi^2}{4z_0^2}. \quad (16)$$

In the case  $p \approx 0$ , the solution of eq. (15) reads as

$$a \approx \frac{\pi}{2(z_0 + D/\alpha)}. \quad (17)$$

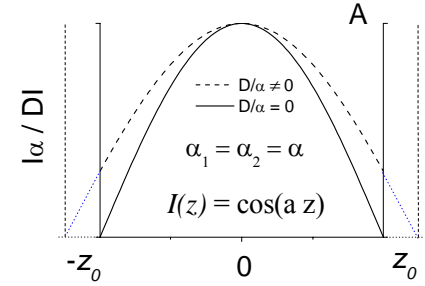
If we assume  $p = 0$  (absence of any mirror at the boundaries), then formula (17) means that the presence of weak mirrors at the boundaries results in effective increase in the thickness of the film (fig. 8, a)

$$z_{eff} = z_0 + D/\alpha. \quad (18) \text{МАРИНА}$$

In the opposite case of strong mirrors:  $p \rightarrow \infty$ ,  $x \rightarrow 0$  and solution of (15) yields:  $a^2 = \alpha/D z_0$ ,  $\bar{a}^2 = \alpha/z_0$ . (19)

Thus in the case of 100% mirrors, the generation condition (12) will depend on film thickness not as  $z_0^{-2}$  (16) but rather as  $z_0^{-1}$  (19). It is important, for example, if pumping is provided electrically through big enough highly reflective electrodes.

As a summary, the solution of the eigen-value problem (9)-(11) for the symmetrical case looks like:  $\bar{a}^2 = \frac{D}{z_0^2} \varphi^2 \left( \frac{D}{\alpha z_0} \right)$ , where the function  $\varphi(\xi)$  is determined from the equation:  $\xi \varphi = ctg(\varphi)$ .



#### 4.2.2. Asymmetrical case

Let us consider now the non-symmetrical case (9)-(11) when  $\alpha_1 \neq \alpha_2$ . The solution of (9) will look as (fig. 8, b):

$$I_z = \cos(az + \psi) \quad (20)$$

The substitution of (20) into the boundary conditions (11), (12) yields a set of equations for determining  $a$  and  $\psi$ . After evaluation one comes to the equation for  $a$  similar to (15):

$$ctg(x) = \frac{(p_1 + p_2)x}{1 - p_1 p_2 x^2 + \sqrt{(1 + p_1^2 x^2)(1 + p_2^2 x^2)}}. \quad (21)$$

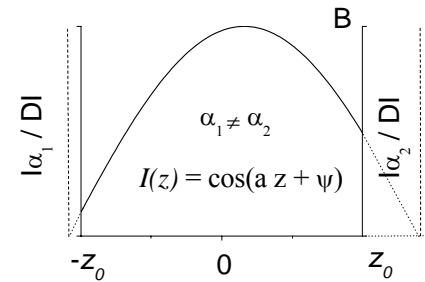


Fig. 8. Solution of z-part in (a) symmetrical and (b) asymmetrical case.

Here, we take:  $x \equiv az_0$ ,  $p_1 \equiv D/\alpha_1 z_0$  and  $p_2 \equiv D/\alpha_2 z_0$ . It is seen that, if  $\alpha_1 = \alpha_2$ , (21) transforms to (15). It can also be shown that from (21) follows one more quite evident fact: if at one of the boundaries, for instance  $z = -z_0$ , we have an ideal mirror, i.e.,  $p_2 \rightarrow \infty$  or, which is just the same,  $(\partial I_z / \partial z)|_{z=-z_0} = 0$ , then the solution of (21) will be  $x = x_s/2$ , where  $x_s$  is the solution of a symmetrical problem with  $\alpha = \alpha_1$ . This means that the existence of an ideal mirror at one of the boundaries doubles the effective thickness of the film.

#### 4.3. Evaluation of the boundary conditions

According to the paper<sup>13</sup> devoted to the theory of light propagation in disordered media the coefficients in the boundary conditions can be estimated as follows:

$$\frac{D}{\alpha} = \frac{2l^*}{3} \frac{1+R}{1-R}, \quad (22)$$

$$R = \frac{3C_2 + 2C_1}{3C_2 - 2C_1 + 2}, \quad (23)$$

where  $l^*$  is the transport mean free path of the light in the scattering medium,

$$C_1 = \int_0^{\pi/2} R(\theta) \sin(\theta) \cos(\theta) d\theta, \quad C_2 = \int_0^{\pi/2} R(\theta) \sin(\theta) \cos^2(\theta) d\theta, \quad (24)$$

here

$$R(\theta) = (R_{\perp}(\theta) + R_{\parallel}(\theta))/2 \quad (25)$$

with  $R_{\perp}(\theta)$ ,  $R_{\parallel}(\theta)$  being the Fresnel reflection coefficients for intensity of light with s- and p- polarizations.

When integrating over the angle of incidence  $\theta$  one should take into account that, if the refractive index of the film is higher than the refractive index of the outer media, the total reflection occurs for all  $\theta \geq \theta_c$ , where  $\theta_c$  is the angle of total reflection. Therefore, the first integration in (24) gives

$$\int_0^{\pi/2} R(\theta) \sin(\theta) \cos(\theta) d\theta = \int_0^{\theta_c} R(\theta) \sin(\theta) \cos(\theta) d\theta + \int_{\theta_c}^{\pi/2} \sin(\theta) \cos(\theta) d\theta \quad \text{and, analogously, for the second integration.}$$

Let us now make some estimations.

If  $n_2 = 2.6$  and  $n_1 = 1$ , then  $\frac{D}{\alpha_1} = \frac{2l^*}{3} \frac{1+R}{1-R} \cong 10.8l^*$ . If  $n_2 = 2.6$  and  $n_3 = 1.5$ , then  $\frac{D}{\alpha_2} = \frac{2l^*}{3} \frac{1+R}{1-R} \cong 3.7l^*$ .

For writing down the generation condition one should find  $x = az_0$ . This number is the root of the transcendental equation (21). To solve this equation we should estimate firstly  $p_1 = D/\alpha_1 z_0$  and  $p_2 = D/\alpha_2 z_0$ . Both of these quantities are proportional to  $(l^*/z_0)$ . Thus, the latter parameter plays a crucial role in the considered problem. If  $l^* \ll z_0$  and reflection at the boundaries is not very high, then  $p_1, p_2 \rightarrow 0$  and  $a \rightarrow \pi/2z_0$ , i.e., as in the case of the zero boundary conditions (16). That is why we took the zero boundary conditions for the radial part<sup>4</sup>. We believe that in the radial problem  $(l^*/r_0) \ll 1$ . If we suppose that in our case  $l^* \approx \lambda$  and, hence, take  $(l^*/z_0) \approx 1$ , then in the considered situation  $p_1 \approx 10.8$  and  $p_2 \approx 3.7$ . The solution of Eq. (21) yields:  $x \approx 0.4$ . That is  $az_0 \approx 0.4$  and  $a \approx 0.4/z_0$ . For the absorbing boundary conditions (16) we have  $a = \pi/2z_0$ . This means that refraction at the boundaries ensures an effective increase in the thickness of the film by  $\pi/(2 \cdot 0.4) = 3.9$  times.

If we put the ideal mirror at the boundary  $z = -z_0$ , instead of the film-glass interface, then the solution for  $x$  will be two times smaller than for the symmetrical problem with  $p_1 = p_2 \approx 10.8$ , that is  $x = 0.3/2 = 0.15$ . It corresponds to the effective increase of the thickness of the film by  $\pi/(2 \cdot 0.15) = 10.5$  times. The generation condition for the gain,

$g = vl_{gain}$ , reads as  $g \geq D \left( \frac{2.4^2}{r_0^2} + \frac{x^2}{z_0^2} \right)$ ,  $r_0$  is the beam radius,  $z_0 = d/2$ ,  $d$  is the thickness of the film,  $D = vl^*/3$ ,  $v$  is

the light velocity in the medium,  $l^*$  is the transport mean free path of the light in the scattering medium. For the generally employed absorbing boundary conditions  $x = \pi/2$  results of the experiments are fitted in fig. 9. Partially

reflective boundaries decrease the value of  $x$ . The developed theory allows calculating the value of  $x$  knowing refractive indexes of the film and the value of the parameter  $(l^*/z_0)$ .

Note that the above considerations are inaccurate for single-photon pumping because variable separation and, hence, the solution become more sophisticated. However, the apparent similarity of the curves in fig. 9 a and 9 b suggests that the solution will have no qualitative differences.

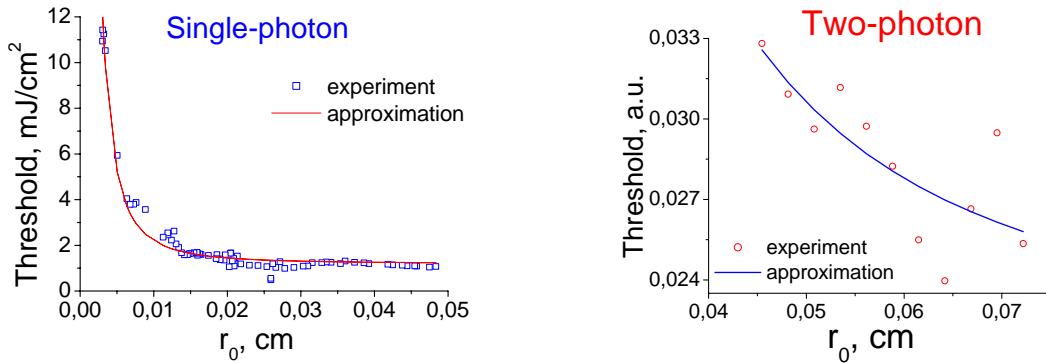


Fig. 9. Theoretical dependences of laser action threshold on laser beam radius: single-photon pumping on the left, and two-photon on the right.

## CONCLUSION

The random laser effect predicted by Letokhov in 1968 is well known in colloidal and microsized media from the experimental point of view. But studies in the case of nanostructured materials are not so well advanced because of the lack of pure and size controlled nanocluster materials. In this communication, we considered excellent optical properties of well controlled nanostructured ZnO thin films prepared by the pulsed laser ablation method. These properties allow easy observation of random laser effect under two-photon excitation. Two-photon pumping of a ZnO thin film was observed and studied for the first time. Comparison of two- and single-photon pumping was carried out. Emission intensity, spectral width and spectral position of random laser emission as a function of pump laser fluence have been studied for the same ZnO film.

A strong increase of the laser action threshold with decreasing laser beam radius has been observed. The value of threshold fluence tends to constant with increasing area of the spot.

Nonlinear transmission of the pumping light in case of two-photon pumping has been observed and discussed.

Theoretical consideration of the effect of boundary conditions on lasing in the disordered film under two-photon excitation has been performed.

## ACKNOWLEDGEMENTS

This work was supported by the project of cooperation between the University Paris 13 (Villetaneuse, France), Université de la Méditerranée (Marseille, France) and the Institute of Applied Physics RAS (Nizhny Novgorod, Russia) "Réseau Formation - Recherche - Europe Centrale et Orientale" and the Program of the Presidium of the Russian Academy of Sciences "Femtosecond optics and physics of superstrong laser fields."



## REFERENCES

1. G. I. Petrov, V. Shcheslavskiy, and V. V. Yakovlev, I. Ozerov, E. Chelnokov, and W. Marine, "Efficient Third-harmonic Generation in a Thin Nanocrystalline Film of ZnO." *Appl. Phys. Lett.*, **83**, pp. 3993-3995, 2003.
2. D. Wiersma, "The smallest random laser." *Nature*, **406**, pp. 132-133, 2000.
3. V. S. Letokhov, "Light generation by a scattering medium with a negative resonant absorption." *Sov. Phys. JETP*, **26**, pp. 835-840, 1968.
4. X. H. Wu, A. Yamilov, H. Noh, and H. Cao, E. W. Seelig and R. P. H. Chang, "Random lasing in closely packed resonant scatterers", *J. Opt. Soc. Am. B*, **21**, pp. 159-167, 2004.
5. I. Ozerov, D. Nelson, A. V. Bulgakov, W. Marine and M. Sentis, "Synthesis and laser processing of ZnO nanocrystalline thin films." *Appl. Surf. Sc.*, **212-213**, pp. 349-352, 2003.
6. I. Ozerov, M. Arab, V. I. Safarov, W. Marine, S. Giorgio, M. Sentis and L. Nanai, "Enhancement of exciton emission from ZnO nanocrystalline films by pulsed laser annealing." *Applied Surface Science*, **226**, pp. 242-248, 2004.
7. K. Postava, H. Sueki, M. Aoyama, T. Yamaguchi, Ch. Ino, Y. Igasaki, and M. Horie, "Spectroscopic ellipsometry of epitaxial ZnO layer on sapphire substrate." *J. of Appl. Phys.*, **87**, pp. 7820-7824, 2000. <http://www.luxpop.com/>
8. W. Marine, "Laser processing of nano objects for microelectronic applications." Agenda of 6th International EULASNET Meeting, 6-7 May 2004, Marseille, France. <http://www.bit.ac.at/eulasnet/6th/marine.pdf>
9. V.S. Dnepropetrovskiy, V.I. Klimov, M.G. Novikov, "Stimulated emission and Mott transition in the direct semiconductor." *JETP. Lett. rus.*, **51**, pp. 219-222, 1990.
10. D. Anglos et al., "Random laser action in organic-inorganic nanocomposites." *J. Opt. Soc. Am. B*, **21**, p. 208, 2004.
11. Y. Ling, H. Cao, A. L. Burin, M. A. Ratner, X. Liu, and R. P. H. Chang, "Investigation of random lasers with resonant feedback." *Phys. Rev. A.*, **64**, p. 063808, 2001.
12. A. L. Burin, H. Cao, M. A. Ratner, "Random Lasers With Coherent Feedback." *IEEE Journal of Selected Topics in QE*, **9**, p. 124, 2003.
13. J. X. Zhu, D. J. Pine, and D. A. Weitz, "Internal reflection of diffusive light in random media." *Phys. Rev. A.*, **44**, p. 3948, 1991.